Journal of Sound and Vibration (2001) **244**(3), 453–479
doi:10.1006/jsvi.2000.3485, available online at http://www.idealibrary.com on IDEAL®

BIFURCATIONS OF APPROXIMATE HARMONIC BALANCE SOLUTIONS AND TRANSITION TO CHAOS IN AN OSCILLATOR WITH INERTIAL AND ELASTIC SYMMETRIC NONLINEARITIES

A. A. Al-Qaisia

Department of Mechanical Engineering, Faculty of Engineering and Technology, University of Jordan, Amman 11942, *Jordan. E-mail: alqaisia@ju.edu.jo*

AND

M. N. Hamdan

Department of Mechanical Engineering, King Fahd University of Petroleum and Minerals, Dhahran, Saudi Arabia

(*Received* 6 *September* 2000)

The local stability of approximate periodic solutions and period-doubling bifurcations in a harmonically forced non-linear oscillator with symmetric elastic and inertia non-linearities are studied analytically and numerically. Approximate principal resonance solutions are first obtained using a two-term harmonic balance and then a consistent second order stability analysis of the associated linearized variational equation is carried out using approximate methods to predict zones of symmetry breaking leading to period-doubling bifurcation and chaos. The results of the present work, which follows the analysis approach presented by Szemplinska-Stupnika (1986 *International Journal of Nonlinear Mechanics* **23**, 257–277; 1987 *Journal of Sound and Vibration* **113**, 155–172) are verified for selected system parameters by numerical simulations using methods of qualitative theory, and good agreement was obtained between the analytical and numerical results. Finally, a criterion for the period-doubling bifurcation is proposed analytically, for this type of oscillator, and compared with computer simulation results that predict the true period-doubling bifurcation and chaos boundaries. © 2001 Academic Press

1. INTRODUCTION

The route to chaos from regular period motion (or from chaos to regular periodic motion) through a sequence of period-doubling bifurcation in non-linear oscillators with single equilibrium positions has been the subject of many analytical and numerical investigations, e.g. references [1–10]. These studies and others have shown that this route to (or from) chaos can be adequately described by making use of approximate analytical methods to study various instabilities of approximate periodic solutions along with a computer simulation using methods of the qualitative theory. By making use of variational Hill-type equations to examine various instabilities of corresponding approximate periodic solutions, these studies have shown that it is possible to determine and describe with fair accuracy, if any, the zones of period-doubling bifurcations on the resonance curves of individual harmonic solutions. Then methods of qualitative theory with the aid of digital computer simulations were used in these studies to determine the locations of chaotic motion zones, which are preceded by period-doubling bifurcations. Szemplinska-Stupnika [1, 2] used this

0022-460X/01/280453 + 27 $35.00/0 © 2001 Academic Press

approach in connection with the harmonic balance method to describe the period-doubling bifurcations in a single equilibrium Duffing oscillator with asymmetric hardening non-linearity [2] and the symmetry breaking and then period-doubling bifurcations in single equilibrium symmetric Duffing oscillators with softening non-linearity [1]. It is to be noted that for an oscillator with asymmetric non-linearities, an approximate periodic solution is asymmetric which usually contains a bias and both even and odd harmonics. For such oscillators the stability analysis of the variational equation corresponding to an asymmetric periodic solution shows that even to first order the asymmetric periodic solution can undergo period-doubling bifurcations, i.e., period-doubling bifurcations are very likely in oscillators with asymmetric non-linearities. The results of the analysis presented in reference [2], show that for an asymmetric Duffing oscillator the chaotic motion appears in a narrow zone which is preceded by a wider period-doubling zone close to the theoretical stability limit of the $\frac{1}{2}$ subharmonic resonance, i.e., in the neighborhood of the frequency where the $\frac{1}{2}$ resonance curve has a vertical tangent. On the other hand, symmetric non-linear oscillators of the hardening type do not, as a general rule, admit, at least in the first approximation asymmetric solution which is necessary for period-doubling bifurcations, i.e., the stability analysis of the variational Hill-type equation corresponding to an approximate periodic solution in a symmetric non-linear oscillator shows that an approximate solution can undergo period doubling provided that it is asymmetric (e.g., see references [1, 2] for more details). The results presented in references [2, 3, 9, 10] for the classical Duffing oscillator and the Duffing–Ueda oscillator with hardening non-linearities obtained using a combination of harmonic balance and numerical simulations, show that for symmetric non-linear oscillators of the hardening type the transition to (or from) chaos is a sharp one and is associated with the loss of stability of the third superharmonic resonant response. In this case the chaotic motion appears at frequencies well below the principal resonance, i.e., in the region which is not adequately described by a first approximate harmonic solution. It is to be noted that the results presented in references [2, 4, 8–10] and in many other studies, indicate that for an asymmetric or a symmetric non-linear oscillator of the hardening type with single equilibrium position oscillator the chaotic motion is always associated with the loss of stability of secondary resonance (super-, ultrasuper-, sub- or ultrasub-harmonic). That is, in such oscillators, the chaotic motion forms a transition zone which separates two periodic solutions having different periods (i.e., having different topological properties). On the other hand, in the symmetric Duffing oscillator with softening-type elastic non-linearity, numerical and analytical results presented in references [1, 5, 7, 11–13] show that in this oscillator the chaotic motion is preceded by a sequence of period doubling and appears near the peak of the principal resonance curve. Using a combined harmonic balance and computer simulation, Szemplinska-Stupnika [1] showed that the stability analysis of the first approximate harmonic solution for this oscillator can predict the symmetry-breaking and period-doubling bifurcations provided that higher order instabilities of the corresponding variational Hill-type equation are examined. It is to be noted that, unlike the classical symmetric Duffing oscillator with hardening non-linearity, the symmetric Duffing oscillator with softening non-linearity can admit in the first approximation, asymmetric solutions which appear in pairs at usually relatively large response amplitude over a narrow frequency band [5]. For example, in order to illustrate a point of interest in the present work, consider the non-linear Duffing oscillator

$$\ddot{u} + \delta\dot{u} + u + \varepsilon u^3 = P\cos(\Omega t + \phi), \tag{1}$$

where δ, ε, P, Ω and ϕ are constants, and $\delta \geqslant 0$. This Duffing oscillator is of the hardening type when $\varepsilon > 0$ and is of the softening type when $\varepsilon < 0$. The constant phase ϕ was added to

the forcing term so that one may obtain a response in which the fundamental harmonic contains a cosine term only. Using the harmonic balance method, an asymmetric periodic solution to equation (1) in the first approximation takes the form

$$u(t) = A_0 + A_1 \cos(\Omega t), \tag{2}$$

where A_0 is a constant bias and A_1 is constant amplitude. Substituting equation (2) and its derivatives into equation (1), ignoring harmonic terms higher than the fundamental which arise, and balancing the remaining harmonics leads to the following set of three non-linear algebraic equations for the unknowns A_0, A_1, Ω and ϕ which define the steady state frequency response:

$$A_1(1 - \Omega^2 + 3\varepsilon A_0^2 + \tfrac{3}{4}\varepsilon A_1^2) = P\cos\phi, \tag{3}$$

$$\delta\Omega A_1 = P\sin\phi, \tag{4}$$

$$A_0\,(1 + \varepsilon A_0^2 + \tfrac{3}{2}\,\varepsilon A_1^2) = 0. \tag{5}$$

From equation (5) one can see that there are two possible solutions: the first has $A_0 = 0$ which corresponds to the symmetric solution, and the second is asymmetric for which the bias is given by

$$A_0 = \pm\left[-\frac{1}{\varepsilon}\left(1 + \frac{3}{2}\varepsilon A_1^2\right)\right]^{1/2} \tag{6}$$

From equation (6) one can easily see that a pair of asymmetric solutions in the first approximation, i.e., a pair of non-zero real values of the bias A_0, may exist for a certain range of amplitude and system parameters only when $\varepsilon < 0$, e.g., when the oscillator is of the softening type. The steady state A_1–Ω relation for the asymmetric solution may be obtained by adding the square of equation (3) to that of equation (4) and using equation (6) whereby one obtains

$$\Omega^2 = -\left(2 + \frac{\delta^2}{2} + \frac{15}{4}\varepsilon A_1^2\right) \pm \left[\frac{\delta^4}{4} + \delta^2\left(2 + \frac{15}{4}\varepsilon A_1^2\right) + \left(\frac{P}{A_1}\right)^2\right]^{1/2}, \quad \varepsilon \leqslant 0. \tag{7}$$

On the other hand, the steady state A_1–Ω relation corresponding to the first approximate symmetric solution for the oscillator in equation (1) is obtained by adding the square of equation (3) to that of equation (4) with $A_0 = 0$. This leads to

$$\Omega^2 = \left(1 - \frac{\delta^2}{2} + \frac{3}{4}\varepsilon A_1^2\right) \pm \left[1 + \frac{\delta^4}{4} - \delta^2\left(1 + \frac{3}{4}\varepsilon A_1^2\right) + \left(\frac{P}{A_1}\right)^2\right]^{1/2}, \tag{8}$$

which is valid for both the softening and hardening oscillators. The frequency response curves obtained using equations (7) and (8) are shown in Figure 1 for the softening case $\varepsilon = -1$ with $\delta = 0{\cdot}4$ and $P = 0{\cdot}23$ which was the subject of numerous detailed investigations (e.g., references [1, 5, 8, 11, 13, 14]). Also shown in this figure are the unstable regions of the above approximate harmonic solutions. The boundaries of these unstable regions were determined by following the procedure in references [1, 2, 15] as outlined in section 2, e.g., by analyzing the associated linearized variational Hill-type equation using the harmonic balance method. These results, which were also reported in references [1, 5, 8, 11, 14], show that the resonance curves of the asymmetric solution intersect those of the symmetric solution near the region of chaotic motion, which lies in the zone where the

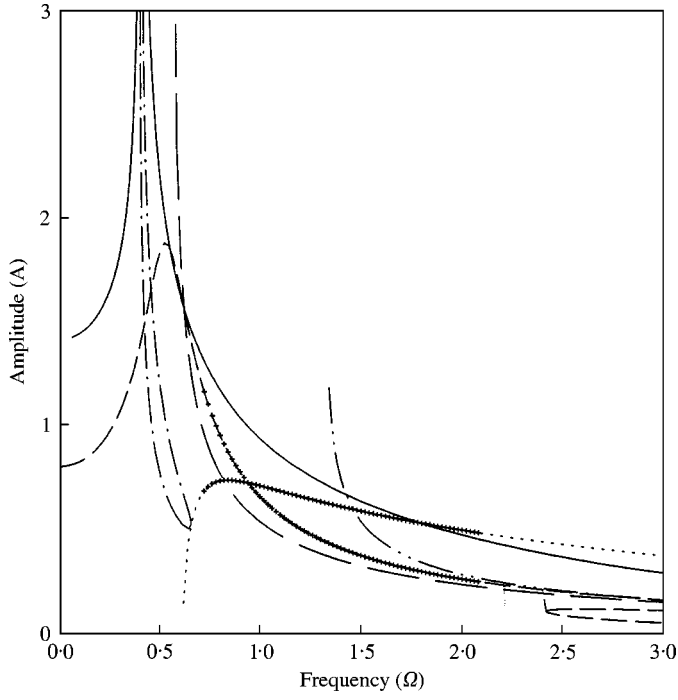

Figure 1. Steady state frequency response (SSFR), first order stability (1st stab.), second order stability (2nd stab.), biased solution and its stability using a single term only. $P = 3{\cdot}5$, $\varepsilon_1 = 10$, $\varepsilon_2 = 1$ and $\delta = 0{\cdot}5$: ——, SSFR; –·–·–·, 1st stab.; —··—, 2nd stab.; ·····, A_0; – – – – – A_1; + + + + +, unstable A_0 and A_1; ——, A_{+ve}. Positive value of A in the symmetric solution at which A_0 in the biased solution has a non-zero real value, calculated from equation (28)."

principal resonance curves of the symmetric first approximate solution may enter the second unstable region of the corresponding variational Hill-type equation. Furthermore, these asymmetric solutions are only stable within this narrow zone [5]. It is to be noted that although the interest here is not specifically in the frequency response characteristics and stability of approximate solution of softening oscillators in the form given by equation (1), analytical and numerical simulation results presented in reference [14] indicate that the qualitative nature of the approximate harmonic balance solution changes, for certain ranges of system parameters, if one uses a two-mode (i.e., fundamental plus third) harmonic balance solution instead of a single-mode (i.e., only fundamental) harmonic balance solution. The results of stability analysis of the approximate harmonic solutions presented in reference [14] and in more detail in reference [15], show that erroneous (i.e., qualitatively incorrect) instability boundaries and type can be obtained if the level of approximation in the solution of the associated linearized variational equation is not consistent with (i.e., the same as) that of the approximate solution.

Dooren [13] introduced a numerical procedure to study the transition from regular periodic motion to chaotic behavior of the Duffing oscillator in equation (1) with softening non-linearity. The procedure used is based on the computation of accurate higher order approximate periodic solution of Galerkin's type in conjunction with the corresponding stability analysis of the first variational equation.

Zavodney *et al.* [16] investigated the response of a single-degree-of-freedom system with quadratic and cubic non-linearities to a principal parametric resonance. They used the method of multiple-time-scales (MMS) to determine the second order modulation of the

amplitude and phase, and verified these equations by integrating the governing equations using an analog computer "to obtain a global bifurcation diagram in the excitation amplitude–excitation frequency plane" and a digital computer "to obtain Poincaré maps and transition from a smooth basin to a fractal basin of attraction".

Awrejcewicz and Mrozowski [17] discussed the chaotic dynamics of a particular non-linear oscillator having Duffing-type stiffness, Van der Pol damping and dry friction. They utilized an averaging technique to obtain information regarding the bifurcation behavior of the vibrating oscillator and analyzed numerically, the chaotic behavior of the oscillator for parameters near bifurcation curves. Also, they studied the effect of dry friction on the behavior of strange chaotic attractor.

Nayfeh and Sanchez [7] also studied the periodic and non-periodic response of the Duffing oscillator in equation (1) with softening non-linearity. They used a second order multiple-time-scale (MMS) with reconstitution to obtain an approximate second order solution in conjunction with the Floquet theory to analyze the associated variational equation, which was linearized about the predicted second order approximate solution. The calculated Floquet multipliers were used to guide the generation of the bifurcation diagram in the parameter space of interest. They showed that the proposed scheme is capable of predicting symmetry-breaking and period-doubling bifurcation as well as jumps to either bounded or unbounded motions. The results obtained are validated using analog and digital computer simulations, which show chaos and unbounded motions.

Asfar and Masoud [18] investigated the phenomenon of period-doubling bifurcation with the Duffing oscillator with negative linear stiffness with the aid of approximate analytical methods and computer simulation. They use the Hill-type variational equation with the Floquet theory to find the type of subharmonic instabilities that are responsible for the occurrence of period doublings in the considered system and they proposed a threshold criterion for the onset of period doubling and compared it with the computer simulation.

In the present work, which is motivated by the work in references [1, 2], the main concern is with approximate analysis, aided with a computer simulation, of the stability, symmetry-breaking and period-doubling bifurcations leading to chaos of approximate harmonic solutions of the harmonically driven non-linear oscillators having single equilibrium positions and described by the general non-dimensional form

$$\ddot{u} + \delta\dot{u} + u + \varepsilon_1 (u^2\ddot{u} + u\dot{u}^2) + \varepsilon_2 u^3 = P\cos(\Omega t), \tag{9}$$

where δ, ε_1, ε_2, P and Ω are constant positive parameters. The interest here is focused on the cases where the oscillator in equation (9) is not weakly non-linear, i.e., when the displacement u is of order unity, ε_1 and/or ε_2 are not necessarily small compared to unity. In the above oscillator, which has a single equilibrium position at $u = 0$, the two non-linear terms inside the parentheses are of inertial type having a net softening effect, while the last non-linear term is of hardening type. Thus, depending on the relative values of ε_1 and ε_2 the characteristics of the frequency response curves of this oscillator may be of softening or hardening type. These characteristics were studied in reference [19] using the harmonic balance method and two versions of the second order perturbation multiple-time-scale with reconstitution method. The results in reference [19] show that the two-mode harmonic balance method yields quantitatively fairly accurate and qualitatively accurate solutions even when the oscillator is relatively strongly non-linear, while the first approximate solution obtained using a single-mode harmonic balance or the perturbation MMS method as well as the second order approximate solution obtained using MMS with reconstitution may lead to qualitatively incorrect frequency response characteristics. The interest in the above oscillator lies in the physical systems that it can model, such as the in-plane flexural

vibrations of an inextensible beam element [20, 21]. Depending on the range of its parameters, the above oscillator may exhibit primary and secondary (sub- or super-harmonic) resonance responses as well as irregular (chaotic) behavior. The focus of interest here, which is motivated by the work in references [1, 2], is to use the methods of approximate theory in conjunction with numerical simulation using the methods of qualitative theory such as phase plane plots, Poincaré maps, frequency spectrums and Lyapunov exponents, to determine for a selected range of system parameters the boundaries of period-doubling bifurcations and chaotic zones relative to the principal resonance curves. Based on the results presented in reference [19] the two-term harmonic balance method is used to obtain the approximate fundamental symmetric solution, and to analyze to second order the stability of the associated linearized variational Hill-type equation. The harmonic balance method is also used in this work to study the steady state frequency response curves and stability of the asymmetric solution of the non-linear oscillator.

2. APPROXIMATE SYMMETRIC SOLUTIONS

An approximate solution to the oscillator in equation (9) may be obtained using the harmonic balance method which does not place a restriction on the order of magnitudes of non-linear terms relative to linear ones, i.e., ε_1 and ε_2 need not be small compared to 1. For convenience, equation (9) is rewritten in terms of a new time scale $T = \Omega t$, so that it becomes

$$\Omega^2\ddot{u} + \Omega\delta\dot{u} + u + \varepsilon_1\Omega^2u^2\ddot{u} + \varepsilon_1\Omega^2u\dot{u}^2 + \varepsilon_2u^3 = P\cos(T + \phi), \tag{10}$$

where dots are now derivatives with respect to the new time T, and the unknown constant phase ϕ has been added to the harmonic excitation so that one can obtain a harmonic balance solution in which the fundamental has a cosine term only. A two-term approximate symmetric solution to equation (10) can be obtained by substituting

$$u(T) = A_1\cos T + A_3\cos 3T + B_3\sin 3T \tag{11}$$

into equation (10), where A_1, A_3, B_3 and ϕ can be determined by the harmonic balance method (HB), and solving the set of non-linear algebraic equations for A_1, A_3, B_3 and ϕ. Results for the steady state response using a two-term harmonic balance method (2THB) have been presented in reference (19) for different values of the parameters δ, ε_1, ε_2 and P. For convenience, in Appendix A, the application of the harmonic balance method using a single term (SHB) and two terms (2THB), from which one can obtain the steady state response curves, is shown.

3. STABILITY ANALYSIS OF SYMMETRIC HARMONIC BALANCE SOLUTIONS

The stability analysis of the approximate harmonic balance solution in equation (11) may be carried out by introducing a small perturbation $v(T)$ to the assumed solution (11), i.e., by substituting

$$u(T) = A_1\cos T + A_3\cos 3T + B_3\sin 3T + v(T) \tag{12}$$

into equation (10), for the sake of brevity and to demonstrate the procedure used in obtaining results for the stability. The stability analysis will be examined by using a single

term only in the assumed solution, i.e., by substituting $u(T) = A\cos T + v(T)$ into equation (11). This leads to the following non-linear variational equation:

$$\ddot{v}\Omega^2\left(1 + \varepsilon_1\frac{A^2}{2} + \varepsilon_1 v^2 + 2\varepsilon_1 vA\cos T + \varepsilon_1\frac{A^2}{2}\cos 2T\right)$$
$$+ \dot{v}(\delta\Omega - 2\varepsilon_1\Omega^2 Av\sin T - \varepsilon_1\Omega^2 A^2\sin 2T)$$
$$+ v\left(\frac{3}{2}\varepsilon_2 A^2 + 1 - \varepsilon_1\Omega^2\frac{A^2}{2} + \varepsilon_1\Omega^2\dot{v}^2 + \frac{3}{2}\varepsilon_2 A^2\cos 2T - \frac{3}{2}\varepsilon_1\Omega^2 A^2\cos 2T\right)$$
$$+ \varepsilon_1\Omega^2 A^2\dot{v}^2\cos T + v^2 A\cos T(3\varepsilon_2 - \varepsilon_1\Omega^2) + \varepsilon_2 v^3 = \frac{A^2}{4}(2\varepsilon_1\Omega^2 - \varepsilon_2)\cos 3T. \quad (13)$$

Results from substituting equation (12) into equation (11) are shown for convenience in Appendix B.

The stability is governed by the linearized version of equation (13). In addition, the excitation term on the right-hand side is deleted, because it has no influence on the stability; this leads to the following Hill-type equation:

$$\ddot{v}\Omega^2\left(1 + \varepsilon_1\frac{A^2}{2}(1 + \cos 2T)\right) + \dot{v}(\delta\Omega - \varepsilon_1\Omega^2 A^2\sin 2T)$$
$$+ v\left(1 + \frac{A^2}{2}(3\varepsilon_2 - \varepsilon_1\Omega^2) + \frac{3}{2}A^2\cos 2T(\varepsilon_3 - \varepsilon_1\Omega^2)\right) = 0. \quad (14)$$

Then by virtue of the Floquet theory, a particular solution of the linearized variational equation LVE (14), is sought in the form [1]

$$v(T) = \mathrm{e}^{\beta T}\,\eta(T), \quad (15)$$

where β is defined as the characteristic exponent and $\eta(T)$ is a periodic function with periods T and $T/2$. The solution of $v(T)$ is stable (respectively, unstable) if the real part of β is negative (positive); and the real part of β is zero on the boundary between stable and unstable regions [15].

The approximate theory of the Hill-type equations allows one to assume functions $\eta_{\mathrm{I}}(T)$ and $\eta_{\mathrm{II}}(T)$ as truncated Fourier series, so that at the stability boundaries, i.e., $\beta = 0$. the disturbances are sought as

$$\eta_{\mathrm{I}}(T) = v(T)_{\beta=0} = \sum_m^{\infty} b_m\cos(mT + \psi_m) = b_{mc}\cos(mT) + b_{ms}\sin(mT), \quad m = 1,3,5,\cdots,\infty, \quad (16)$$

$$\eta_{\mathrm{II}}(T) = v(T)_{\beta=0} = b_0 + \sum_m^{\infty} b_m\cos(mT + \psi_m) = b_0 + b_{mc}\cos(mT) + b_{ms}\sin(mT),$$
$$m = 2,4,6,\cdots,\infty. \quad (17)$$

The instabilities of type I (first order stability) are those which bring odd harmonic components to the system response, while type II (second order stability) gives a build-up of the even harmonic component [1].

The first and second order unstable regions can be predicted by substituting equations (16) and (17) into the LVE (14) and using the harmonic balance method. This leads to an infinite set of linear homogeneous equations (b_{mc} and b_{ms}, $m = 1, 3, 5, \cdots, \infty$ for analysis I) or (b_0, b_{mc} and b_{ms}, $m = 2, 4, 6, \cdots, \infty$ for analysis II). These equations can be expressed in matrix form as $\mathbf{Ax} = \mathbf{0}$, where $\mathbf{x}$ is one of the two column vectors $(\cdots, b_{ic}, b_{is}, \cdots)^{\mathrm{T}}$, and $(b_0, \cdots, b_{ic}, b_{is}, \cdots)^{\mathrm{T}}$; $\mathbf{A}$-is the characteristic matrix. Nontrivial solutions for b_m exist only when the determinant (Δ) of the characteristic matrix, vanishes. This determinant depends on β, thus $\Delta(\beta) = 0$ provides the characteristic equation for β. The stability conditions become $\Delta(\beta = 0)$ is positive (respectively, negative) in a stable (unstable) region, and $\Delta(\beta = 0) = 0$ at the boundary between the stable and unstable regions [15].

To determine the boundaries of the first unstable region "i.e., analysis I" according to the above procedure, one may substitute as a first approximation

$$\eta_{\mathrm{I}}(T) = v(T)_{\beta=0} = b_{1c}\cos(T) + b_{1s}\sin(T) \tag{18}$$

into equation (14) and applying the harmonic balance method to obtain the following set of algebraic equations for (b_{1c}, b_{1s}):

$$\begin{bmatrix} 1 - \Omega^2 + \dfrac{A^4}{4}(3\varepsilon_2 - 2\varepsilon_1\Omega^2) & -\delta\Omega \\ \delta\Omega & 1 - \Omega^2 + \dfrac{A^2}{4}(9\varepsilon_2 - 6\varepsilon_1\Omega^2) \end{bmatrix} \begin{Bmatrix} b_{1c} \\ b_{1s} \end{Bmatrix} = \begin{Bmatrix} 0 \\ 0 \end{Bmatrix}. \tag{19}$$

Non-trivial solutions for b_{1c}, b_{1s} exist only when the determinant of the coefficient matrix in (19) vanishes, which gives the following relation:

$$\Omega^4\left(1 + 2\varepsilon_1 A^2 + \frac{3}{4}\varepsilon_1^2 A^4\right) + \Omega^2\left(\delta^2 - 2 - A^2(3\varepsilon_2 + 2\varepsilon_1) - \frac{9}{4}\varepsilon_1\varepsilon_2 A^4\right) + \left(1 + 3\varepsilon_2 A^2 + \frac{27}{16}\varepsilon_2^2 A^4\right) = 0. \tag{20}$$

Solving the last equation for Ω^2 gives the boundaries of the first order unstable region. The boundaries of the second unstable region "i.e., analysis II", which may give rise to period-doubling bifurcation (PDB), can be obtained by substituting the following equation as a first approximation:

$$\eta_{\mathrm{II}}(T) = v(T)_{\beta=0} = b_0 + b_{2c}\cos(2T) + b_{2s}\sin(2T), \tag{21}$$

into equation (14) and applying the harmonic balance method to obtain a set of algebraic equations,

$$\begin{bmatrix} 1 + \dfrac{A^2}{2}(3\varepsilon_2 - \varepsilon_1\Omega^2) & 0 & \dfrac{3A^2}{4}(\varepsilon_2 - \varepsilon_1\Omega^2) \\ 0 & 1 - 4\Omega^2 + \dfrac{A^2}{2}(3\varepsilon_2 - 5\varepsilon_1\Omega^2) & -2\delta\Omega \\ \dfrac{3A^2}{2}(\varepsilon_2 - \varepsilon_1\Omega^2) & 2\delta\Omega & 1 - 4\Omega^2 + \dfrac{A^2}{2}(3\varepsilon_2 - 5\varepsilon_1\Omega^2) \end{bmatrix} \begin{Bmatrix} b_0 \\ b_{2s} \\ b_{2c} \end{Bmatrix} = \begin{Bmatrix} 0 \\ 0 \\ 0 \end{Bmatrix}. \tag{22}$$

Non-trivial solutions for b_0, b_{2s}, b_{2c} exist only when the determinant of the coefficient matrix in equation (22) vanishes, which gives the following relation between A and Ω, for certain system parameters δ, ε_1, ε_2:

$$\frac{A^6}{16}(\varepsilon_2^3 - 99\varepsilon_1\varepsilon_2\Omega^2 + 93\varepsilon_1^2\varepsilon_2\Omega^4 - 5\varepsilon_1^3\Omega^6)$$

$$+\frac{A^4}{8}(45\varepsilon_2^2 - \Omega^2(108\varepsilon_2^2 + 114\varepsilon_1\varepsilon_2) + \Omega^4(216\varepsilon_1\varepsilon_2 + 61\varepsilon_1^2) - 44\varepsilon_1^2\Omega^6)$$

$$+\frac{A^2}{2}(9\varepsilon_2 + \Omega^2(12\delta^2\varepsilon_2 - 48\varepsilon_2 - 11\varepsilon_1) + \Omega^4(48\varepsilon_1 + 48\varepsilon_2 - 4\delta^2\varepsilon_1) - 16\varepsilon_1\Omega^6)$$

$$+1 + \Omega^2(4\delta^2 - 8) + 16\Omega^4 = 0 \tag{23}$$

to be satisfied at the stability boundary. Equation (23) can be resolved for A^2 to give the boundaries of the second unstable region and the critical bifurcation value of the amplitude.

4. APPROXIMATE ASYMMETRIC SOLUTIONS AND THEIR STABILITIES

Using the harmonic balance method, an asymmetric periodic solution to equation (10) in the first approximation takes the form

$$u(T) = A_0 + A_1 \cos T, \tag{24}$$

where A_0 is a constant bias and A_1 is the amplitude. Substituting equation (24) and its derivatives into equation (10), one obtains

$$A_1\left[A_0^2(3\varepsilon_2 - \varepsilon_1\Omega^2) + \frac{A_1^2}{4}(3\varepsilon_2 - 2\varepsilon_1\Omega^2) + 1 - \Omega^2\right] = P\ \cos\phi, \tag{25}$$

$$A_1\delta\Omega = P\sin\phi, \tag{26}$$

$$A_0\left[A_0^2\varepsilon_2 + \frac{A_1^2}{2}(3\varepsilon_2 - \varepsilon_1\Omega^2) + 1\right] = 0. \tag{27}$$

For $A_0 \neq 0$, it follows from equation (27) that

$$A_0^2 = \frac{1}{\varepsilon_2}\left[\frac{A_1^2}{2}(\varepsilon_1\Omega^2 - 3\varepsilon_2) - 1\right]. \tag{28}$$

Equations (25), (26) and (28), yield (in terms of A_1 only) the frequency response equation of the system:

$$\left(\frac{225}{16}\varepsilon_2^4 - \frac{75}{4}\varepsilon_1\varepsilon_2^3\Omega^2 + 10\varepsilon_1^2\varepsilon_2^2\Omega^2 - \frac{5}{2}\varepsilon_1^3\varepsilon_2\Omega^6 + \frac{1}{4}\varepsilon_1^4\Omega^8\right)A_1^6$$

$$+\left(15\varepsilon_2^3 - \frac{35}{2}\varepsilon_1\varepsilon_2^2\Omega^2 + \frac{15}{2}\varepsilon_2^2\Omega^2 + 7\varepsilon_1^2\varepsilon_2\Omega^4 - 5\varepsilon_1\varepsilon_2^2\Omega^4 - \varepsilon_1^3\Omega^6 + \varepsilon_1^2\varepsilon_2\Omega^6\right)A_1^4$$

$$+(4\varepsilon_2^2 + \delta^2\Omega^2 - 4\varepsilon_1\varepsilon_2\Omega^2 + 4\varepsilon_2^2\Omega^2 + \varepsilon_1^2\Omega^4 - 2\varepsilon_1\varepsilon_2\Omega^4 + \varepsilon_2^2\Omega^4)A_1^2 = P^2. \tag{29}$$

Steady state resonance curves A_0 and A_1 can be determined from equations (28) and (29) respectively.

The stability of the assumed solution (24), can be examined by using the same procedure followed in the previous section, i.e., by substituting $u(T) = A_0 + A_1 \cos T + v(T)$, into equation (10). This yields the following linearized version of the variational equation:

$$\ddot{v}\Omega^2 \left[1 + \frac{A_1^2}{2}\varepsilon_1 (1 + \cos 2T) + \varepsilon_1 (A_0^2 + 2A_0 A_1 \cos 2T)\right]$$
$$+ \dot{v}\left[\delta\Omega - \varepsilon_1 \Omega^2 (A_1^2 \sin 2T + 2A_0 A_1 \sin T)\right]$$
$$+ v\left[1 + \frac{A_1^2}{2}(3\varepsilon_2 (1 + \cos 2T) - \varepsilon_1 \Omega^2 (1 + 3\cos 2T))\right.$$
$$\left. + 3\varepsilon_2 A_0^2 + 2A_0 A_1 \cos T (3\varepsilon_2 - \varepsilon_1 \Omega^2)\right] = 0. \tag{30}$$

It is clear that equation (30) has two parametric excitations with periods T and $T/2$. To examine the period-doubling bifurcation in the first approximation of the biased solution, one may seek a particular solution at the stability limit as

$$v(T) = b_{1/2} \cos\left(\frac{T}{2} + \psi_{1/2}\right) = b_{1/2)c} \cos\left(\frac{T}{2}\right) + b_{1/2)s} \sin\left(\frac{T}{2}\right). \tag{31}$$

Then, by substituting equation (31) and its derivatives into equation (30), and applying the harmonic balance method and putting the condition of non-trivial solution for $b_{1/2)c}$ and $b_{1/2)s}$, i.e., the determinant of the coefficient matrix equals zero, a relation between the amplitudes (A_0 and A_1) and the frequency Ω to be satisfied at the stability boundary can be obtained, such that

$$\Omega^4 \left(\frac{1}{16} + \frac{\varepsilon_1}{16}(2A_0^2 + 5A_1^2) + \frac{\varepsilon_1^2}{64}(4A_0^4 - 16A_0^2 A_1^2 + 25A_1^4)\right)$$
$$+ \Omega^2 \left(\frac{\delta^2}{4} - \frac{1}{2} - \frac{3\varepsilon_2}{4}(2A_0^2 + A_1^2) - \frac{\varepsilon_1 \varepsilon_2}{8}(12A_0^4 + 15A_0^4) - \frac{\varepsilon_1}{4}(2A_0^2 + 5A_1^2)\right)$$
$$+ \left(1 + 3\varepsilon_2(2A_0^2 + A_1^2) + 9\varepsilon_2^2 \left(A_0^4 + \frac{A_1^2}{4}\right)\right) = 0. \tag{32}$$

For convenience, teh elements of the coefficient matrix are given in Appendix B.

5. COMPUTER SIMULATION, RESULTS AND DISCUSSIONS

The stability analysis of the non-linear oscillator described in equation (10) was verified near the principal resonance zone for selected values of system parameters P, ε_1, ε_2 and δ, using computer simulation and with the aid of time histories, phase plane, Poincaré map and Lyaponuv fractal dimension.

The response of the non-linear oscillator is controlled by two competing softening "$\varepsilon_1 (u^2 \ddot{u} + u\dot{u}^2)$" and hardening "$\varepsilon_2 u^3$" non-linearities, which exhibit fundamentally two different response characteristics [19], depending on the relative value of ε_1 and ε_2.

Results for a softening-type oscillator, i.e., $\varepsilon_1/\varepsilon_2 > 1{\cdot}6$, are presented in Figure (1) and the parameters P, ε_1, ε_2 and δ were chosen to be 3·5, 10, 1, 0·5 respectively.

In Figure 1, the steady state response using the HB method, first and second order unstable regions are obtained using a single term only. In the same figure is also shown the biased solution given in equation (24). One can see from Figure 1 that the first order unstable region intersects the steady state response curve at the vertical tangency point as one may expect "Figure 2", and the second order unstable region intersects the response curve at $\Omega \cong 1{\cdot}43$. To improve the accuracy of the predicted steady state response and stability, results are obtained and shown in Figure 3, for the same oscillator but using two terms for the steady state response, i.e., equation (A8), and stability analysis, i.e., using two terms in the assumed solution of the variational equation (B2) to obtain results for both the first and second order stabilities. In addition, the same figure shows also the biased solution and its stability. Results of the stability analysis "using two terms Figure 3" show that the first order unstable region disappears and the steady state response curve is stable in the resonance area and it seems that the frequency response resembles linear behavior. This behavior was verified numerically and steady state numerical solutions were obtained in the resonance area, as one can see from Figure 4. Stability analysis also shows, that the steady state response curve penetrates into the second unstable region at $1{\cdot}1836 < \Omega < 5{\cdot}8482$, and the biased solution is unstable at $0{\cdot}72 < \Omega < 2{\cdot}07$, at which there is a possibility of period-doubling bifurcation (PDB). It is worth mentioning that the PDB can occur also inside the frequency range $1{\cdot}1836 < \Omega < 5{\cdot}8482$, predicted by the second unstable region.

It was found that by increasing the frequency, the PDB is first observed at $\Omega = 1{\cdot}06$ followed by higher period doublings $4T$ at $\Omega = 1{\cdot}09$ and they develop in chaos at $\Omega = 1{\cdot}095$. The first chaotic zone observed is in the range $1{\cdot}095 < \Omega \leqslant 1{\cdot}29$ and then ends by a $9T$ attractor followed by a $3T$ one. The $3T$ attractor disappears and chaos returns in

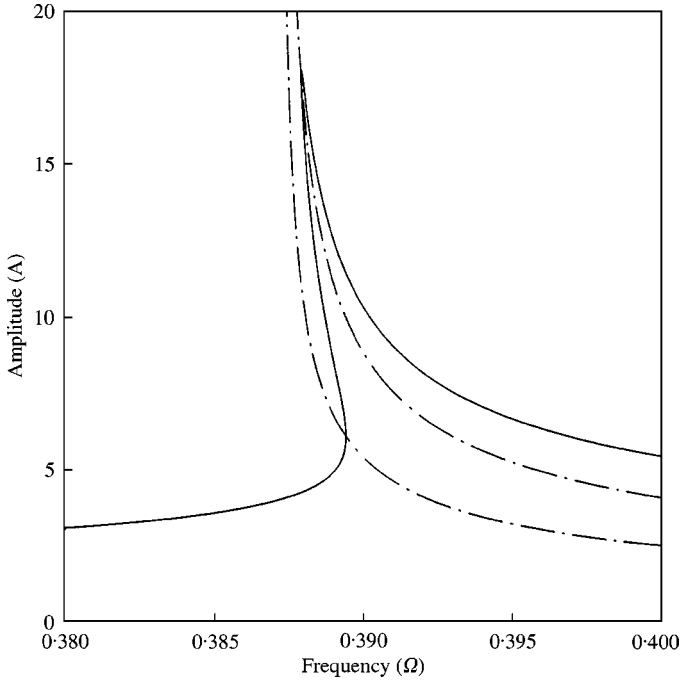

Figure 2. Expanded view of Figure (1): ——, SSFR; – · – · –, 1st stab.

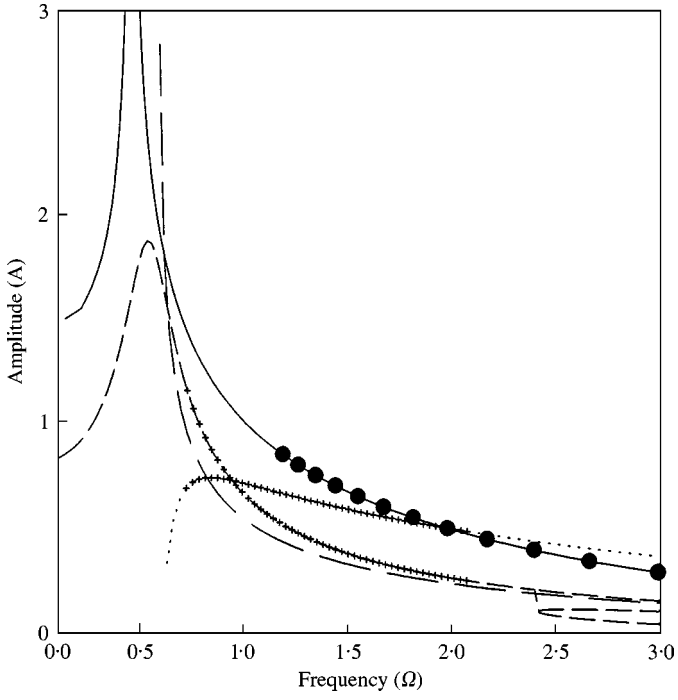

Figure 3. Steady state frequency response (SSFR), first order stability (1st stab.), second order stability (2nd stab.) using two terms. $P = 3{\cdot}5$, $\varepsilon_1 = 10$, $\varepsilon_2 = 1$ and $\delta = 0{\cdot}5$: ———, SSFR. "A_1 of equation (11)", ● 2nd stab., A_0, A_1, A_{+ve} same as in Figure 1.

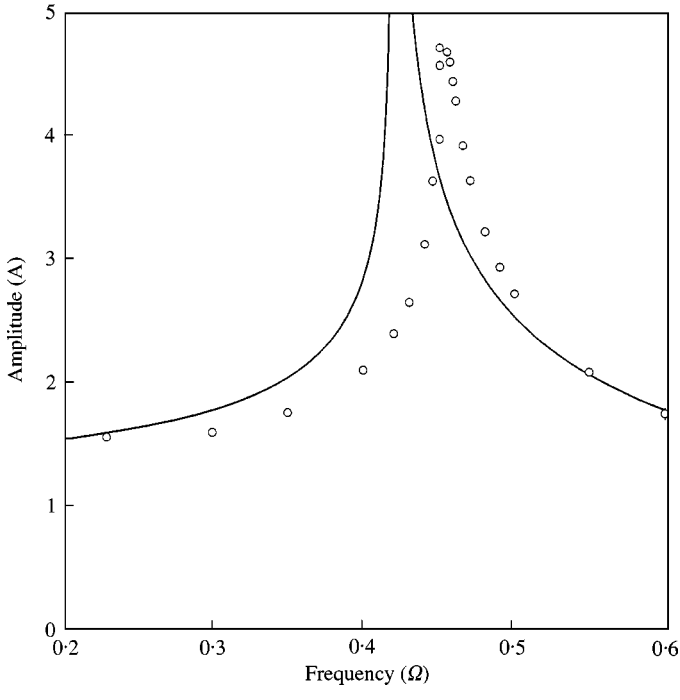

Figure 4. Steady state frequency response (SSFR) using two terms and numerical solution. $P = 3{\cdot}5$, $\varepsilon_1 = 10$, $\varepsilon_2 = 1$ and $\delta = 0{\cdot}5$: ———, SSFR; ○, numerical solution.

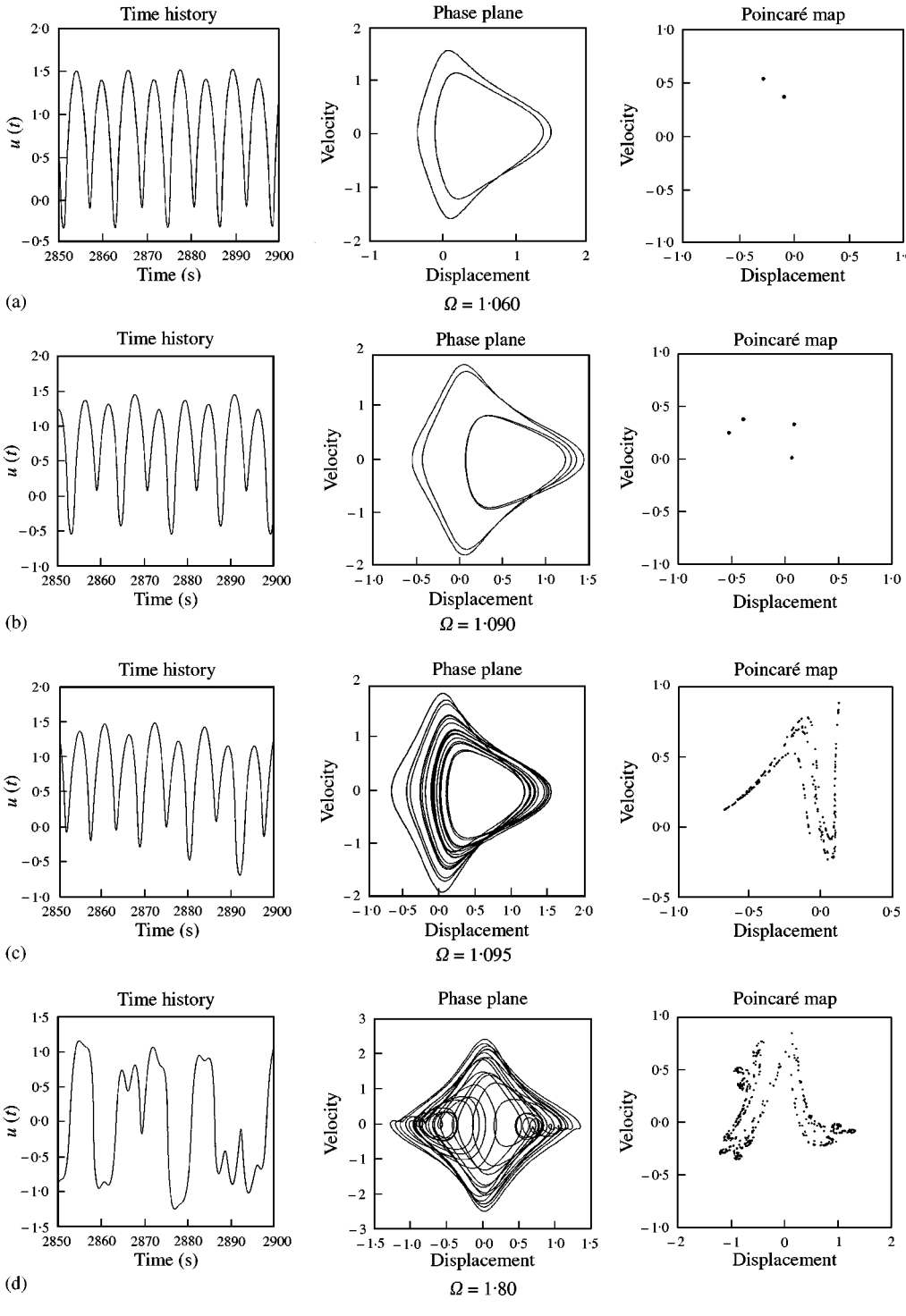

Figure 5. Time history, phase plane and poincaré map. $P = 3{\cdot}5$, $\varepsilon_1 = 10$, $\varepsilon_2 = 1$ and $\delta = 0{\cdot}5$: (a) $\Omega = 1{\cdot}06$; (b) $\Omega = 1{\cdot}09$; (c) $\Omega = 1{\cdot}095$, $\lambda_1 = 0{\cdot}0619$, $\lambda_2 = 0{\cdot}0$, $\lambda_3 = -0{\cdot}1419$ and $d_f = 2{\cdot}436$; (d) $\Omega = 1{\cdot}80$, $\lambda_1 = 0{\cdot}2142$, $\lambda_2 = 0{\cdot}0$, $\lambda_3 = -0{\cdot}2989$ and $d_f = 2{\cdot}717$; (e) $\Omega = 2{\cdot}20$; (f) $\Omega = 2{\cdot}205$, $\lambda_1 = 0{\cdot}2619$, $\lambda_2 = 0{\cdot}0$, $\lambda_3 = -0.3796$ and $d_f = 2{\cdot}690$; (g) $\Omega = 2{\cdot}45$, $\lambda_1 = 0{\cdot}3064$, $\lambda_2 = 0{\cdot}0$, $\lambda_3 = -0{\cdot}4488$ and $d_f = 2{\cdot}683$.

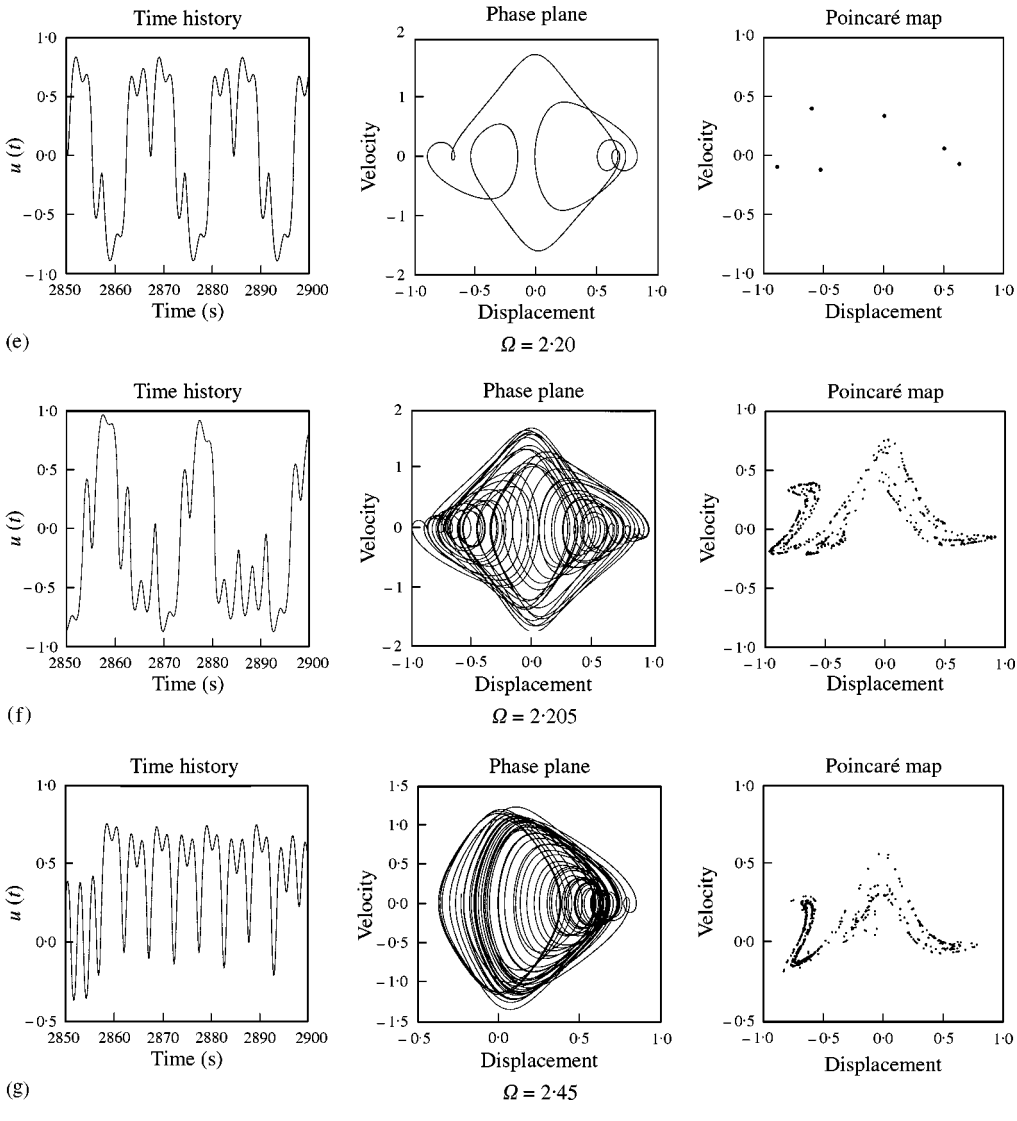

Figure 5. Continued.

the range $1{\cdot}80 \leqslant \Omega \leqslant 2{\cdot}2$, and it ends also by are asymmetric $6T$ attractor. Further investigations showed that the third chaotic zone in the range $2{\cdot}2 < \Omega \leqslant 2{\cdot}5$ ends with higher period doublings $4T$, which is followed by PDB in the range, $2{\cdot}6 < \Omega \leqslant 3{\cdot}0$ and at $\Omega = 3{\cdot}0$ periodicity returns to the system.

In Figures 5, the time histories, phase planes and Poincaré maps are shown for different values of Ω and for the parameters ($P = 3{\cdot}5$, $\varepsilon_1 = 10$, $\varepsilon_2 = 1$, $\delta = 0{\cdot}5$). Results presented in Figures 1 to 4 and with the aid of computer simulations "Figure 5", show that, and as one may expect, the resonance curves of the asymmetric solution intersect those of the symmetric solution near the region of chaotic motion, which lies in the zone where the principal resonance curves of the symmetric solution may enter the second unstable region.

Chaotic behavior of the non-linear oscillator is verified also by another diagnostic tool which is used in dynamical systems, the calculation of Lyapunov exponents. In the present work the Lyapunov exponents are calculated, using the algorithm presented

by Wolf *et al.* [22], from the generated time histories, i.e., by integrating equation (10) using the Runge–Kutta method. Since the dimension of the considered oscillator is 3, the behavior is chaotic if $\lambda_1 > 0$, $\lambda_2 = 0$ and $\lambda_3 < 0$ with $\sum \lambda_i < 0$, where λ_1, λ_2 and λ_3 are the Lyapunov exponents. The fractal dimension of the chaotic attractor can be calculated from the Lyapunov exponents according to the relation [22]

$$d_f = n + \frac{\sum_{i=1}^{n} \lambda_i}{|\lambda_{i+1}|}, \tag{33}$$

where n is defined by the condition, $\lambda_1 + \lambda_2 + \cdots + \lambda_n > 0$. On the presented Poincaré maps, in Figures 5, 7 and 11, that have chaotic behavior, the calculated Lyapunov exponents and the fractal dimensions are shown to be used as a diagnostic tool for chaos.

In the light of the presented results, it can be shown that a criterion that might predict the necessary physical parameters combination for this type of oscillators, for PDB can be proposed. However, PDBs in many non-linear systems occur just before the onset of choas. Therefore, PDBs may be considered often as the lower threshold of chaos [18]. Once the second unstable region intersects with the steady state response curve, i.e., equation (23) is satisfied, one can use this equation which gives critical bifurcation value of the amplitude as a function of the frequency and the system parameters, $A_{cr} \equiv A_{cr}\ (\Omega,\ \varepsilon_1, \varepsilon_2,\ \delta)$. Upon substituting the value of A_{cr} into the frequency response equation (A4), one can obtain the critical value of the forcing parameter [1], such that

$$\left(\frac{1}{16}(9\varepsilon_2^2 - 12\varepsilon_1\varepsilon_2\Omega^2 + 4\varepsilon_1^2\Omega^4)\right)A_{cr}^6 + \left(\frac{3}{2}\,\varepsilon_2\,(1-\Omega^2) + \varepsilon_1\,(\Omega^4 - \Omega^2)\right)A_{cr}^4$$
$$+ (1 + \Omega^2\,(\delta^2 - 2) + \Omega^4)\,A_{cr}^2 = P_{cr}^2. \tag{34}$$

Equation (34) may give the minimum value of the forcing parameter required for period-doubling bifurcation and may be used as a threshold criterion for PDB.

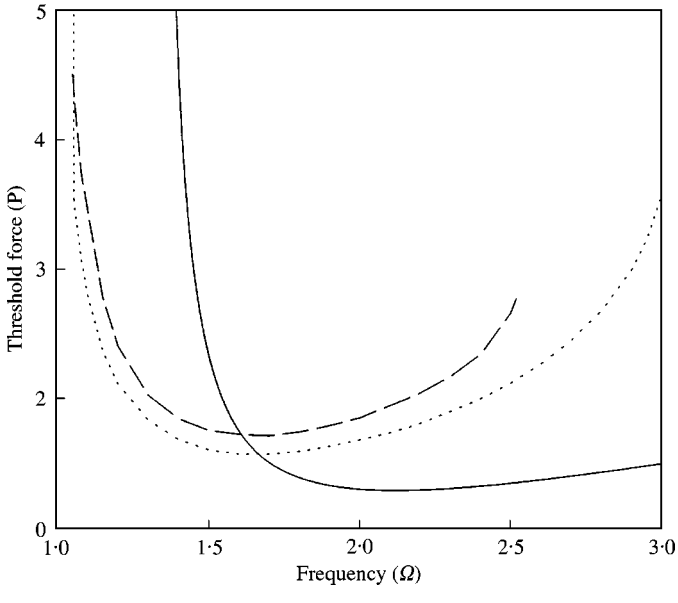

Figure 6. Analytical PDB criterion obtained using equation (34), true PDB and true chaotic boundaries. $P = 3{\cdot}5$, $\varepsilon_1 = 10$, $\varepsilon_2 = 1$ and $\delta = 0{\cdot}5$: ———, Analytical PDB; ·····, true PDB; – – – –, true chaos.

In Figure 6, the proposed criterion is shown with the true boundaries of PDB and chaos for the softening-type non-linear oscillator ($P = 3{\cdot}5$, $\varepsilon_1 = 10$, $\varepsilon_2 = 1$, $\delta = 0{\cdot}5$). The difference between the proposed criterion and the true boundary of PDB is due to the fact that it is calculated by using a single term only in the assumed solution. On the other hand, the boundaries of the true PDB and chaos have the same qualitative characteristics and they give the minimum threshold values for both PDB and chaos.

To verify the results presented in Figure 6 for the true boundaries of PDB and chaos, time histories, phase planes and Poincaré maps are shown in Figure (7), for $\varepsilon_1 = 10$, $\varepsilon_2 = 1$, $\delta = 0{\cdot}5$ and $\Omega = 2{\cdot}0$, at different values of P. The behavior of the oscillator is periodic at $P = 1{\cdot}68$, PDB appears at $P = 1{\cdot}69$ and higher period doublings ($4T$, $8T$) and chaos appear at $P = 1{\cdot}83$, $1{\cdot}85$ and $1{\cdot}86$, respectively.

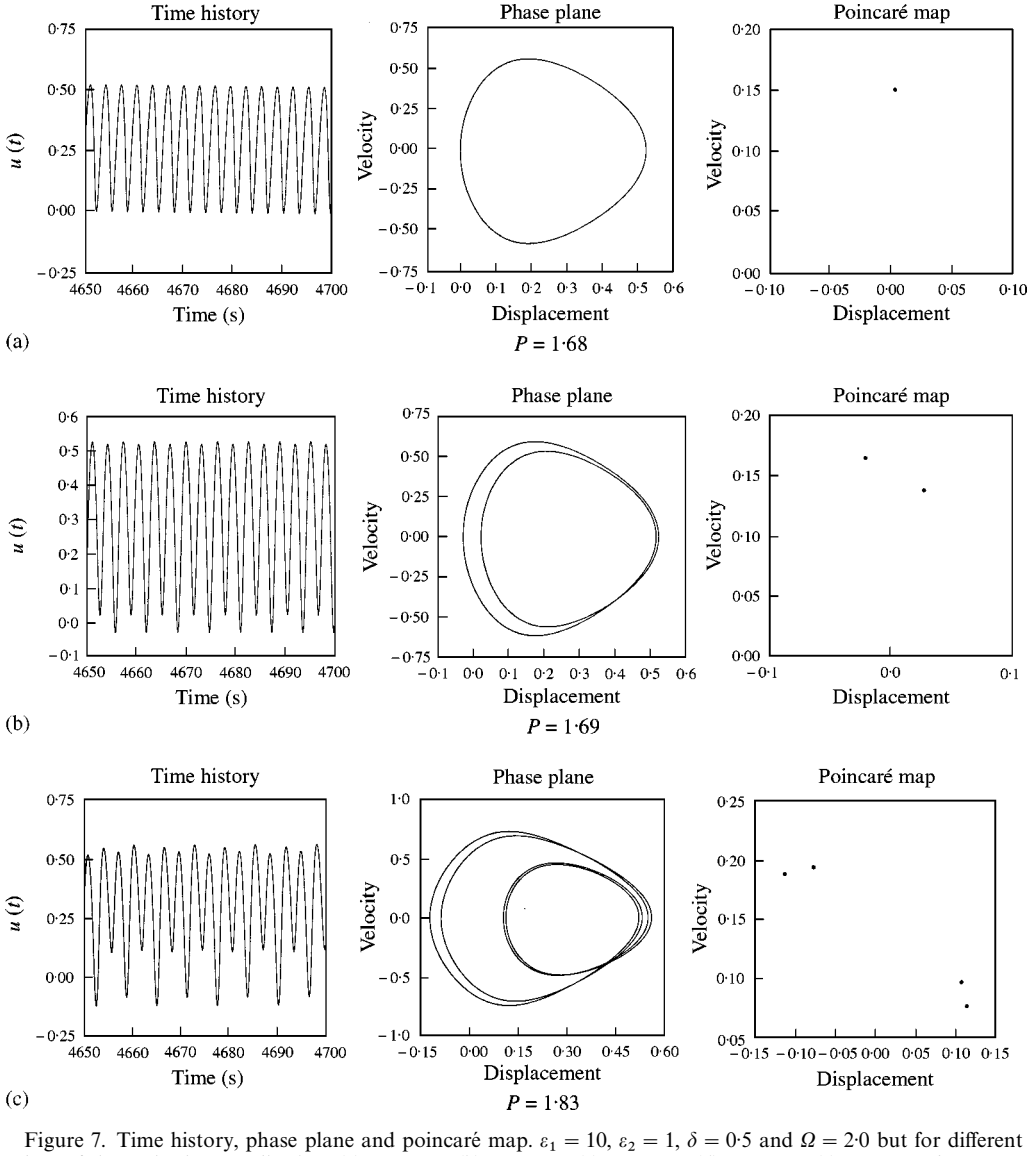

Figure 7. Time history, phase plane and poincaré map. $\varepsilon_1 = 10$, $\varepsilon_2 = 1$, $\delta = 0{\cdot}5$ and $\Omega = 2{\cdot}0$ but for different values of the excitation amplitude P (a) $P = 1{\cdot}68$; (b) $P = 1{\cdot}69$; (c) $P = 1{\cdot}83$; (d) $P = 1{\cdot}85$; (e) $P = 1{\cdot}86$, $\lambda_1 = 0{\cdot}15$, $\lambda_2 = 0{\cdot}0$, $\lambda_3 = -0{\cdot}2332$ and $d_f = 2{\cdot}64322$.

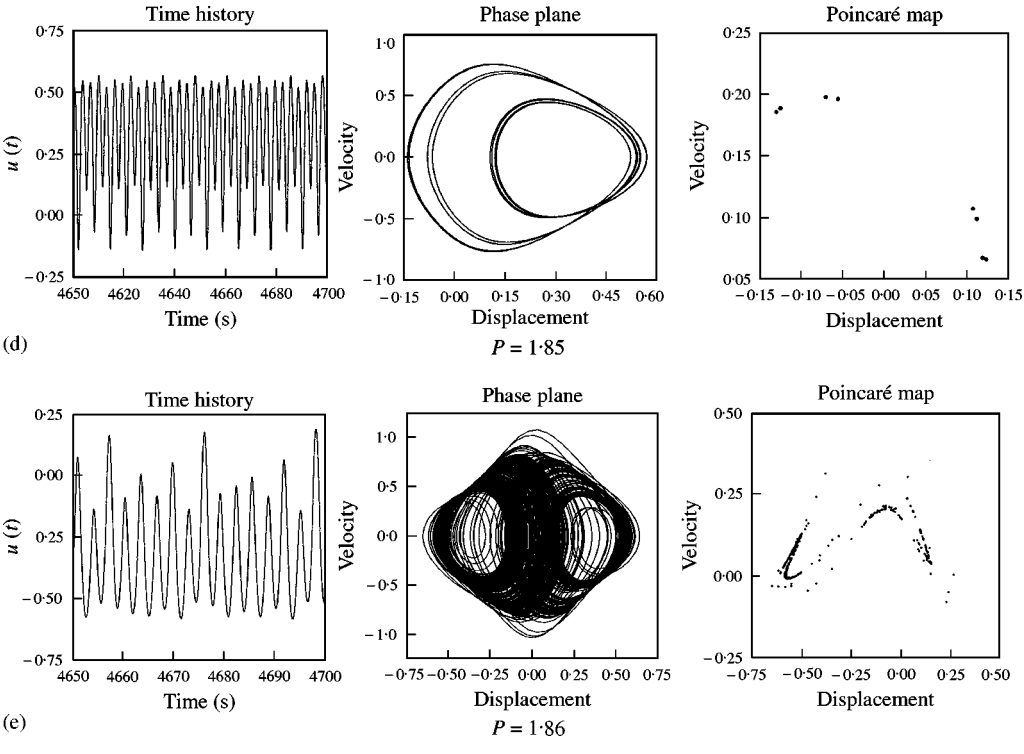

Figure 7. Continued.

In Figure 8, the steady state response, first order and second unstable boundaries, biased solution and stability of the biased solution "asymmetric" are presented for the non-linear oscillator with hardening characteristics, i.e., $\varepsilon_1/\varepsilon_2 < 1{\cdot}6$, for the parameters ($P = 35$, $\varepsilon_1 = 0{\cdot}5$, $\varepsilon_2 = 1$, $\delta = 0{\cdot}1$). The first order unstable region intersects the response curve at the point of vertical tangency and the second unstable region has two boundaries; the first one is located at the superharmonic resonance zone at $0{\cdot}925 < \Omega < 1{\cdot}02$ and the second intersects the response curves at $\Omega = 3{\cdot}30$. In the figure, the asymmetric solution intersects the symmetric one at $\Omega \cong 2{\cdot}55$, i.e., before the steady state response enters the second boundary of the second unstable region.

In Figure 9, results are obtained for the same hardening-type oscillator, i.e., $P = 35$, $\varepsilon_1 = 0{\cdot}5$, $\varepsilon_2 = 1$, $\delta = 0{\cdot}1$, but using two terms for the steady state frequency response and stability analysis. Here the first order unstable region results obtained using two terms has expected characteristics, i.e., intersect the steady state response curve at the point of vertical tangency as shown in Figure 10. The second order stability analysis predicts also two portions: the first one at $0{\cdot}9754 < \Omega \leqslant 1{\cdot}0616$ and the second one at $\Omega \geqslant 3{\cdot}0918$. As one can see, the estimates of the frequency bands of the two portions of the second unstable analysis have been improved when using two terms in the stability analysis. Results obtained from asymmetric solution indicate that the PDB may rise as mentioned before at $\Omega \cong 2{\cdot}55$, and at the frequency band of the first portion of the second unstable region.

Computer simulations inside the first portion, i.e., in the superharmonic resonance area, have predicted three chaotic zones; the first at $0{\cdot}70 < \Omega < 0{\cdot}71$, the second at $0{\cdot}74 < \Omega < 0{\cdot}77$ and the third one at $1{\cdot}019 \leqslant \Omega \leqslant 1{\cdot}080$, PDB at $0{\cdot}79 < \Omega < 0{\cdot}81$ and higher period doubling ($4T$) at $\Omega = 0{\cdot}78$. Computer simulations at values of $\Omega \approx 2{\cdot}55$ where the symmetric solution bifurcates into an asymmetric one "just before the symmetric

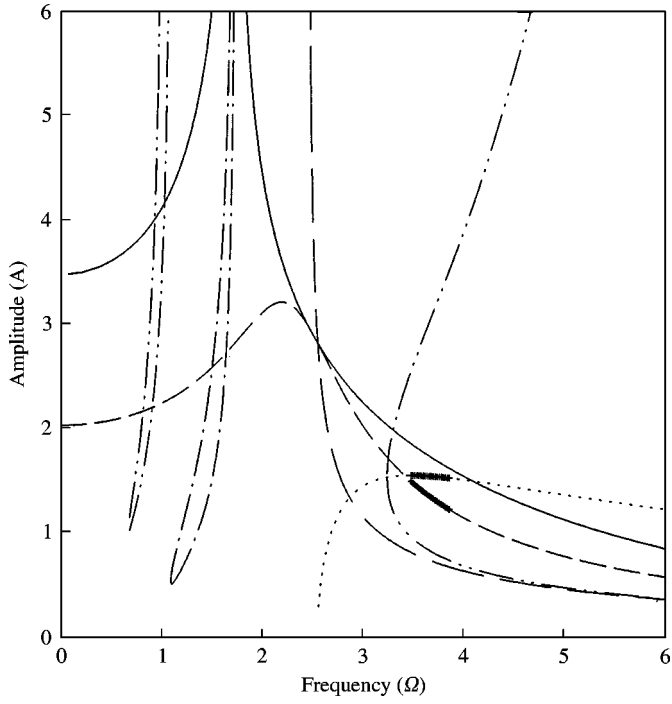

Figure 8. Same as Figure 1, but for the hardening-type oscillator, using a single term only: $P = 35$, $\varepsilon_1 = 0{\cdot}5$, $\varepsilon_2 = 1$ and $\delta = 0{\cdot}1$.

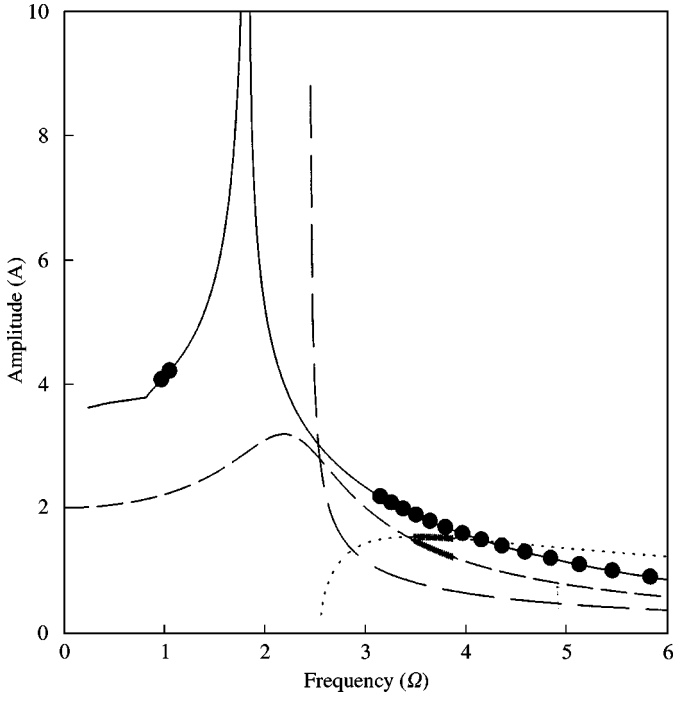

Figure 9. Same as Figure 3, but for the hardening-type oscillator, using two terms: $P = 35$, $\varepsilon_1 = 0{\cdot}5$, $\varepsilon_2 = 1$ and $\delta = 0{\cdot}1$.

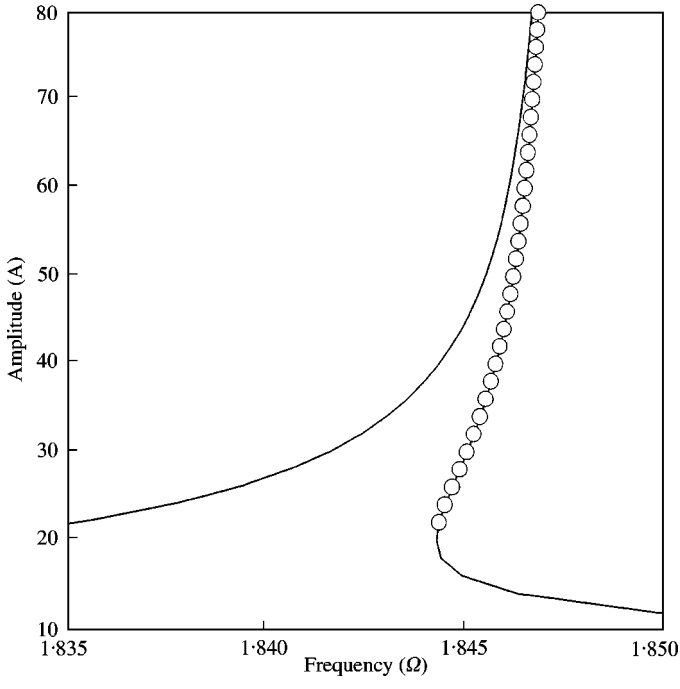

Figure 10. Expanded view of Figure 9: ———, SSFR; ○, 1st stab.

solution enters the second portion of the second unstable region at $\Omega > 3{\cdot}0918$" have shown also some transitions in response of oscillator summarized as follows; PDB in three zones: the first at $2{\cdot}52 < \Omega < 2{\cdot}71$, the second at $3{\cdot}82 < \Omega < 4{\cdot}055$ and the third one at $4{\cdot}58 < \Omega < 4{\cdot}98$, and higher period doublings $8T$ at $\Omega = 4{\cdot}6$ and $16T$ at $\Omega = 2{\cdot}72$.

In Figure 11, time histories, phase planes and poincaré maps for the hardening oscillator are shown for $P = 35$, $\varepsilon_1 = 0{\cdot}5$, $\varepsilon_2 = 1$, $\delta = 0{\cdot}1$ and for some selected values of Ω which simulate different behaviors of the hardening-type oscillator.

6. CONCLUSIONS

The results presented in this work indicate that for the type of non-linear oscillators governed by equation (10), two-terms harmonic solutions of the steady state frequency response and second order stability analysis of the associated linearized variational Hill type equation may predict with good accuracy the portions on the steady state frequency response at which the period-doubling bifurcation (PDB) may rise.

It has been shown that the resonance curves of the asymmetric solution intersect those of the symmetric solution before the symmetric solutions penetrate into the second unstable region, regardless of the characteristic type of the oscillator, i.e., softening or hardening. In addition, it has been shown that at the point of intersection between asymmetric and symmetric solutions, i.e., when A_0 in the biased solution has non-zero real value, the symmetric solution bifurcates into an asymmetric one and the PDB appears in this area and in some cases this PDB develops into chaos.

A criterion for the PDB is presented analytically for this type of non-linear oscillators, i.e., with two competing softening "$\varepsilon_1 (u^2\ddot{u} + u\dot{u}^2)$" and hardening "$\varepsilon_2 u^3$" non-linearities. The boundaries of the true PDB and chaos are obtained numerically according to the

information obtained from stability analysis. These boundaries have the same qualitative characteristics and give the minimum threshold value for PDB and chaos, and it can be used to avoid the PDB and chaotic behavior of this type of oscillator for certain combinations of system parameters. The difference between the calculated and the true PDB boundaries results from neglecting the third harmonic component in the assumed solution used in calculating the critical excitation amplitude P_{cr}, inside the second unstable region.

First order stability results obtained suggest that a more detailed analysis is required, i.e., the analysis which uses some or all of the harmonics used in the assumed solution or analysis which uses some higher harmonics which are not included in the assumed solution, in specific for the softening-type oscillator, which is beyond the scope of the present work.

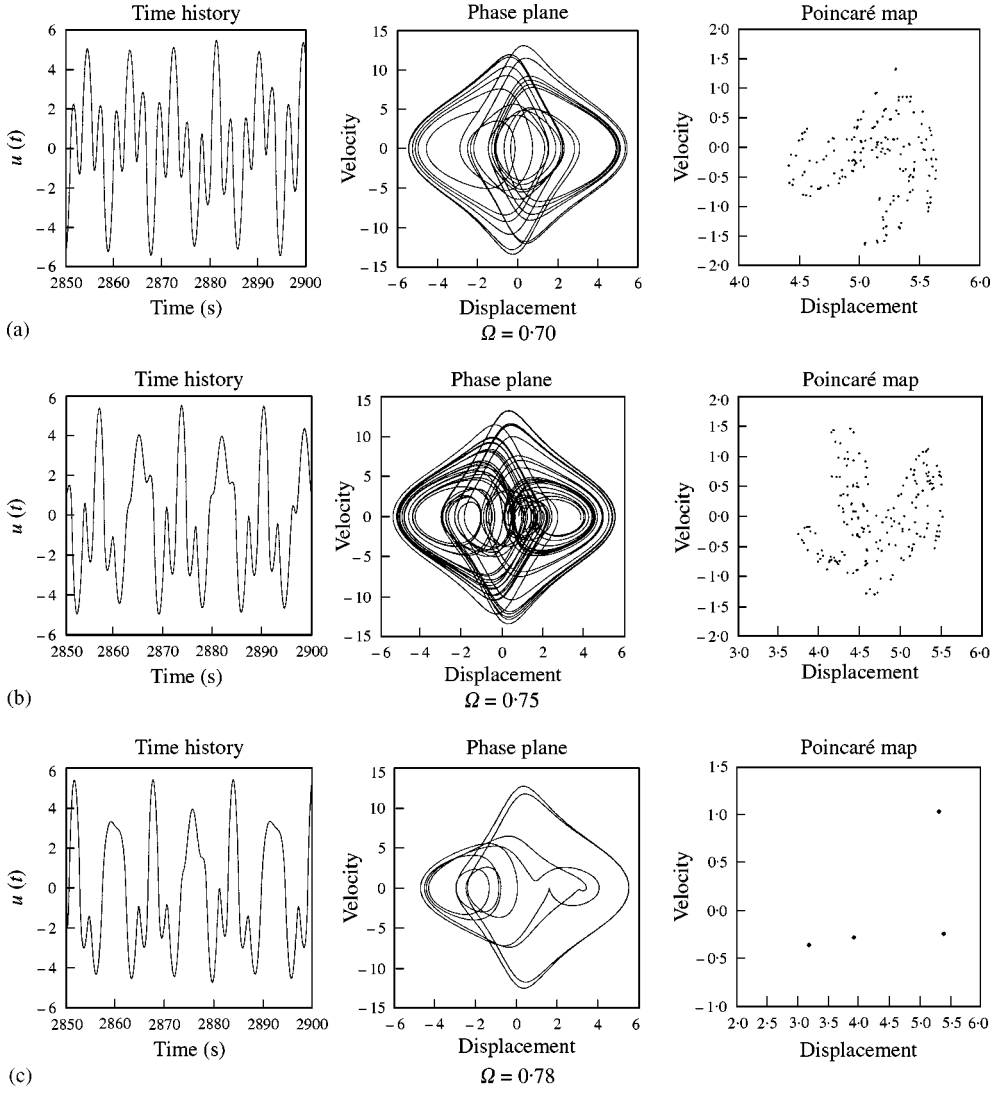

Figure 11. Time history, phase plane and Poincaré map. $P = 35$, $\varepsilon_1 = 0{\cdot}5$, $\varepsilon_2 = 1$, $\delta = 0{\cdot}5$: (a) $\Omega = 0{\cdot}70$, $\lambda_1 = 0{\cdot}0929$, $\lambda_2 = 0{\cdot}0$, $\lambda_3 = -0{\cdot}1105$ and $d_f = 2{\cdot}840$; (b) $\Omega = 0{\cdot}75$, $\lambda_1 = 0{\cdot}1385$, $\lambda_2 = 0{\cdot}0$, $\lambda_3 = -0{\cdot}1599$ and $d_f = 2{\cdot}866$; (c) $\Omega = 0{\cdot}78$; (d) $\Omega = 0{\cdot}80$; (e) $\Omega = 1{\cdot}03$, $\lambda_1 = 0{\cdot}0901$, $\lambda_2 = 0.0$, $\lambda_3 = -0{\cdot}1068$ and $d_f = 2{\cdot}844$.

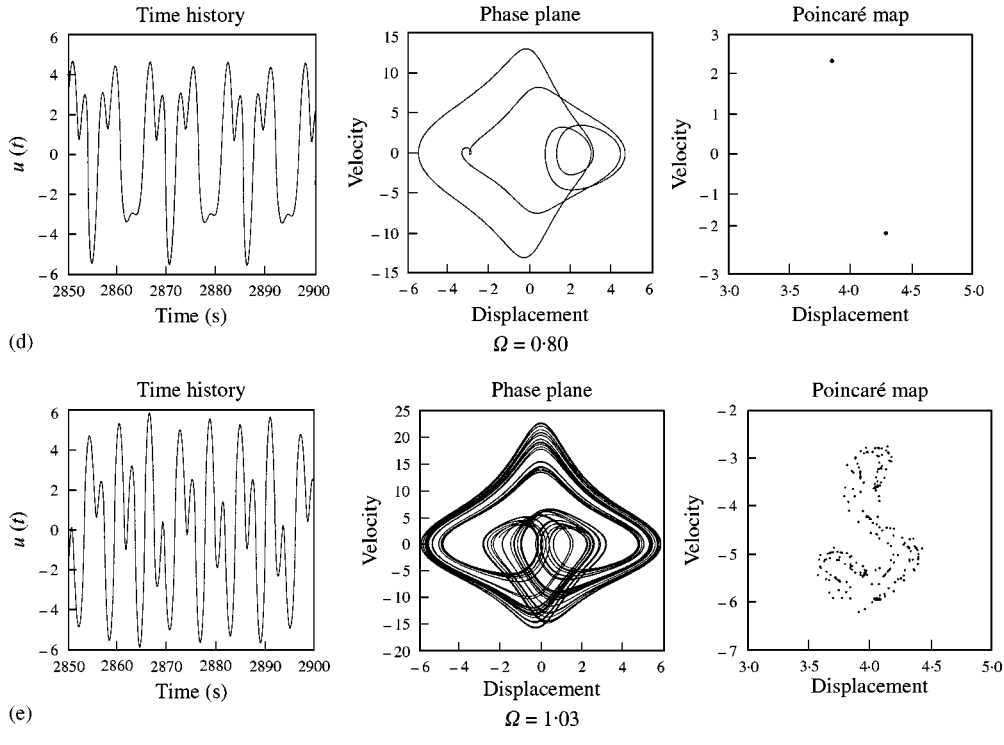

Figure 11. Continued.

ACKNOWLEDGMENT

The authors would like to acknowledge the support of both the Deanship of Scientific Research, University of Jordan, Amman-Jordan and King Fahd University of Petroleum and Mineral, Dhaharan-Saudi Arabia.

REFERENCES

1. W. SZEMPLINSKA-STUPNIKA 1986 *International Journal of Nonlinear Mechanics* **23**, 257–277. Bifurcations of harmonic solution leading to chaotic motion in the softening type Duffing's oscillator.
2. W. SZEMPLINSKA-STUPNIKA 1987 *Journal of Sound and Vibration* **113**, 155–172. Secondary resonance and approximate models of rout to chaotic motion in non-linear oscillators.
3. W. SZEMPLINSKA-STUPNIKA and J. BAJKOWSKI 1986 *International Journal of Non-Linear Mechanics* **21**, 401–419. The 1/2 Subharmonic resonance and its transition to chaotic motion in a non-linear oscillator.
4. J. C. HUANC, Y. H. KAO, C. S. WANG and Y. GOU 1989 *Physics Letters A* **136**, 131–138. Bifurcation structure of the Duffing oscillator with asymmetric potential well.
5. K. L. LIU and K. YOUNG 1986 *Journal of Mathematics and Physics* **27**, 502–506. Stability of forced nonlinear oscillators via Poincare map.
6. JHERATH and K. FESSER 1987 *Physics Letters A* **120**, 265–268. Mode expansions and bifurcations in nonlinear single-well oscillators.
7. A. H. NAYFEH and N. E. SANCHEZ 1989 *International Journal of Non-linear Mechanics* **24**, 483–497. Bifurcations in a forced softening Duffing oscillator.
8. Z. RAHMAN and T. D. BURTON 1986 *Journal of Sound and Vibration* **110,** 363–380. Large amplitude primary superharmonic reasonances in the Duffing oscillator.
9. W. SZEMPLINSKA-STUPNIKA 1994 *Journal of Sound and Vibration* **178**, 276–284. A discussion of an analytical method of controlling chaos in Duffing oscillator.

10. A. HASSAN 1994 *Journal of Sound and Vibration* **172**, 513–526. On the third superharmonic resonance in the Duffing oscillator.
11. B. A. HUBERMAN and J. P. CRUTCHFIELD 1979 *Physical Review Letters* **43,** 1743–1747. Chaotic states of anharmonic systems in periodic fields.
12. R. RATY, J. VON BOEHM and H. M. ISOMAKI 1984 *Physical Letters A* **103**, 289–292. Absence of inversion-symmetric limit cycles of even periods and chaotic motion of Duffing oscillator.
13. R. VAN DOOREN 1988 *Journal of Sound and Vibration* **23**, 327–339. On the transition from regular to chaotic behavior in the Duffing oscillator.
14. M. N. HAMDAN and D. T. BURTON 1993 *Journal of Sound and Vibration* **166**, 255–266. On the steady state response and stability of non-linear oscillators using harmonic balance.
15. A. HASSAN 1996 *Nonlinear Dynamic* **10**, 105–133. On the local stability analysis of the approximate harmonic balance solutions.
16. L. D. ZAVODNEY, A. H. NAYFEH and N. E. SANCHEZ 1989 *Journal of Sound and Vibration* **129**, 417–442. The response of a single-degree-of-freedom system with quadratic and cubic non-linearities to a principal parametric resonance.
17. J. AWREJCEWICZ and J. MROZOWSKI 1989 *Journal of Sound and Vibration* **89**, 89–100. Bifurcation and chaos of a particular Van Der Pol–Duffing oscillator.
18. K. R. ASFAR and K. K. MASOUD 1992 *Transactions of American Society of Mechanical Engineers Journal of Vibration and Acoustics* **144**, 489–494. On the period-doubling bifurcations in the Duffing's oscillator with negative linear stiffness.
19. A. A. AL-QAISIA and M. N. HAMDAN 1999 *Journal of Sound and Vibration* **223**, 49–71. On the steady state response of oscillators with static and inertia non-linearities.
20. A. A. AL-QAISIA, B. AL-BEDOOR and M. N. HAMDAN 2000 *Shock and Vibration* **7**, 179–194. On the steady state response of a cantilever beam partially immersed and carrying an intermediate mass.
21. M. N. HAMADAN and N. H. SHABANEH 1997 *Journal of Sound and Vibration* **199**, 711–736. On the large amplitude vibration of a restrained uniform beam carrying an intermediate mass.
22. A. WOLF, J. B. SWIFT, H. L. SWINNNEY and J. A. VASTANO 1985, *Physica D* **16**, 285–317. Determining Lyapunov exponent from a time series.

APPENDIX A: HARMONIC BALANCE SOLUTION

A.1. SINGLE TERM HARMONIC SOLUTION (SHB)

According to the HB method, an approximate solution of equation (10), takes the form

$$u(T) = A\cos T, \tag{A1}$$

where A is the steady state response amplitude. Substituting equation (A1) into equation (10), neglecting third harmonics that arise, and equating coefficients of first harmonics, one obtains the following equations:

$$\left(\frac{3}{2}\varepsilon_2 - \frac{\varepsilon_1}{2}\Omega^2\right) A^3 + (1 - \Omega^2)\, A = P\cos\phi, \tag{A2}$$

$$\Omega\delta A = P\sin\phi. \tag{A3}$$

The steady state frequency response is obtained by squaring and adding equations (A2) and (A3) and solving for Ω^2 as a function of A; this yields the steady state frequency response:

$$\Omega^4(4\varepsilon_1^2A^6 + \varepsilon_1A^4 + A^2) + \Omega^2\left((\delta^2 - 2)A^2 - (\tfrac{3}{2}\varepsilon_2 + \varepsilon_1)\, A^4 - \tfrac{12}{16}\,\varepsilon_1\varepsilon_2A^6\right)$$

$$+ (A^2 + \tfrac{3}{2}\varepsilon_2A^4 + \tfrac{9}{16}\varepsilon_2^2A^6) = P^2. \tag{A4}$$

Equation (A4) can be written in the form

$$\Omega^2 = R_1 \pm \sqrt{R_1^2 - R_2}, \tag{A5}$$

where

$$R_1 = -\left(\delta^2 - \frac{3}{2}\varepsilon_2 A^2 - \frac{3}{4}\varepsilon_1\varepsilon_2 A^4 - 2 - \varepsilon_1 A^2\right)\Big/\left(2 + 2\varepsilon_1 A^2 + \frac{\varepsilon_1^2 A^4}{2}\right), \tag{A6}$$

$$R_2 = \left(\frac{9}{16}\varepsilon_2^2 A^4 + \frac{3}{2}\varepsilon_2 A^2 + 1 - \frac{P^2}{A^2}\right)\Big/\left(1 + \varepsilon_1 A^2 + \frac{\varepsilon_1^2 A^4}{4}\right). \tag{A7}$$

Equation (A5) yields two real solutions for Ω provided that the radical term is real and less than R_1; a single real solution is obtained when the radical term is zero or greater than R_1, and no real solution exists when $R_1^2 - R_2 < 0$.

A.2. TWO-TERM HARMONIC SOLUTION (2THB)

In order to improve the accuracy of SHB approximation one includes higher harmonics in the assumed solution in equation (A1). In this work, only one more term is added to this equation, whereby the two-term approximation, having the same period as the excitation, to the steady state solution of the system in equation (10) with odd non-linearities takes the form

$$u(T) = A_1 \cos T + A_3 \cos 3T + B_3 \sin 3T. \tag{A8}$$

Substituting equation (A8) and its derivatives into equation (10) and using the same procedure followed previously and neglecting the higher order harmonics, one obtains the following coupled non-linear algebraic equations for A_1, A_3, B_3 and the phase ϕ:

$$\tfrac{3}{4}\varepsilon_2 A_1^3 + \tfrac{3}{4}\varepsilon_2 A_1^2 A_3 + \tfrac{3}{2}\varepsilon_2 A_1 A_3^2 + \tfrac{3}{2}\varepsilon_2 A_1 B_3^2 + A - A\Omega^2 - \frac{\varepsilon_1}{2}\Omega^2 A^3$$

$$- \tfrac{3}{2}\varepsilon_1\Omega^2 A_1^2 A_3 - 5\varepsilon_1\Omega^2 A_1^2 A_3 - 5\varepsilon_1\Omega^2 A_1^2 B_3 = P\cos\phi, \tag{A9}$$

$$\tfrac{3}{4}\varepsilon_2 A_1^2 B_3 - \Omega\delta A_1 - \tfrac{3}{2}\varepsilon_1\Omega^2 A_1^2 B_3 = -P\sin\phi. \tag{A10}$$

$$\tfrac{3}{2}\varepsilon_2 A_1^2 B_3 + \tfrac{3}{4}\varepsilon_2 A_3^2 B_3 + \tfrac{3}{4}\varepsilon_2 B_3^3 + B_3 - 3A_3\delta\Omega - 9\Omega^2 B_3$$

$$- 5\varepsilon_1\Omega^2 A_1^2 B_3 - \tfrac{9}{2}\varepsilon_1\Omega^2 A_3^2 B_3 - \tfrac{9}{2}\varepsilon_1\Omega^2 B_3^3 = 0, \tag{A11}$$

$$\frac{\varepsilon_2}{4}A_1^3 + \frac{3}{2}\varepsilon_2 A_1^3 A_3 + \frac{3}{4}\varepsilon_2 A_3^2 + \frac{3}{4}\varepsilon_2 A_3 B_3^2 + A_3 + 3B_3\delta\Omega - 9A_3\Omega^2$$

$$- \frac{\varepsilon_1}{2}\Omega^2 A_1^3 - 5\varepsilon_1\Omega^2 A_1^2 A_3 - \frac{9}{2}\varepsilon_1\Omega^2 A_3^2 - \frac{9}{2}\varepsilon_1\Omega^2 A_3 B_3^2 = 0. \tag{A12}$$

These equations may be expressed in a more convenient from as follows. First, squaring and adding equations (A9) and (A10) and solving for Ω^2 leads to

$$a\Omega^4 + b\Omega^2 + c = 0, \tag{A13}$$

where

$$a = 1 + A_1^2\varepsilon_1 + 3\varepsilon_1 A_1 A_3 + 10\varepsilon_1 A_3^2 + 10\varepsilon_1 B_3^2 + \tfrac{1}{4}\varepsilon_1 A_1^4 + \tfrac{3}{2}\varepsilon_1^2 A_1^3 A_3 + \tfrac{29}{4}\varepsilon_1^2 A_1^2 A_3^2$$
$$+ 15\varepsilon_1^2 A_1 A_3^2 + 25\varepsilon_1^2 A_3^4 + \tfrac{29}{4}\varepsilon_1^2 A_1^2 B_3^2 + 15\varepsilon_1^2 A_1 A_3 B_3^2 \to 50\varepsilon_1^2 A_3^2 B_3^2 + 25\varepsilon_1^2 B_3^4,$$
$$b = \delta^2 - \tfrac{3}{2}\varepsilon_2 A_1^2 - \tfrac{3}{2}\varepsilon_2 A_1 A_3 - 3\varepsilon_2 A_3^2 - 3\varepsilon_2 B_3^2 - \tfrac{3}{4}\varepsilon_1\varepsilon_2 A_1^4 - 3\varepsilon_1\varepsilon_2 A_1^3 A_3 - \tfrac{45}{4}\varepsilon_1\varepsilon_2 A_1^2 A_3^2$$
$$- 12\varepsilon_1\varepsilon_2 A_1 A_3^2 - 15\varepsilon_1\varepsilon_2 A_3^4 - \tfrac{45}{4}\varepsilon_1\varepsilon_2 A_1^2 B_3^2 - 12\varepsilon_1\varepsilon_2 A_1 A_3 B_3^2 - 30\varepsilon_1\varepsilon_2 A_3^2 B_3^2$$
$$- 15\varepsilon_1\varepsilon_2 B_2^4 - 2 - \varepsilon_1 A_1^2 - 3\varepsilon_1 A_1 A_3 - 10\varepsilon_1 A_3^2 - 10\varepsilon_1 B_3^2,$$
$$c = \tfrac{9}{16}\varepsilon_2^2 A_1^4 + \tfrac{9}{8}\varepsilon_2^2 A_1^3 A_3 + \tfrac{45}{16}\varepsilon_2^2 A_1^2 A_3^2 + \tfrac{9}{4}\varepsilon_2^2 A_1 A_3^3 + \tfrac{9}{4}\varepsilon_2^2 A_3^4 + \tfrac{45}{16}\varepsilon_2^2 A_1^2 B_3^2 + \tfrac{9}{4}\varepsilon_2^2 A_1 A_3 B_3^2$$
$$+ \tfrac{9}{2}\varepsilon_2^2 A_3^2 B_3^2 + \tfrac{9}{4}\varepsilon_2^2 B_3^4 + \tfrac{3}{2}\varepsilon_2 A_1^2 + \tfrac{3}{2}\varepsilon_2 A_1 A_3 + 3\varepsilon_2 A_3^2 + 3\varepsilon_2 B_3^2 + 1 + 3\varepsilon_1\delta\Omega^3 A_1 B_3$$
$$- \tfrac{2}{3}\varepsilon_2\delta\Omega A_1 B_3 - \frac{P^2}{A_1^2}. \tag{A14}$$

Next, equations (A11) and (A12) are solved implicitly for A_3 and B_3 respectively:

$$B_3 = \frac{[-\tfrac{3}{4}\varepsilon_2 B_3 (A_3^2 + B_3^2) + \tfrac{9}{2}\varepsilon_1\Omega^2 B_3 (A_3^2 + B_3^2) + 3A_3\delta\Omega]}{[\tfrac{3}{2}\varepsilon_2 A_1^2 + (1 - 9\Omega^2 - 5\varepsilon_1\Omega^2 A_1^2)]}, \tag{A15}$$

$$A_3 = \frac{[A_1^3((\varepsilon_1/2)\Omega^2 - \varepsilon_2/4) - \tfrac{3}{4}\varepsilon_2 A_3 (A_3^2 + B_3^2) - 3\delta\Omega B_3 + \tfrac{9}{2}\varepsilon_1\Omega^2 A_3 (A_3^2 + B_3^2)]}{[\tfrac{3}{2}\varepsilon_2 A_1^2 + 1 - 9\Omega^2 - 5\varepsilon_1\Omega^2 A_1^2]}. \tag{A16}$$

Equation (A13) can be written using the form

$$\Omega^2 = R_3 \pm \sqrt{R_3^2 - R_4}, \tag{A17}$$

where R_3 and R_4 can be calculated from equation (A14), so that, $R_3 = (-b/2a)$ and $R_3 = (c/a)$. Equation (A17) has two real solutions provided that $R_3^2 > R_4$ and $\sqrt{R_3^2 - R_4} < R_3$. A single real solution exists provided that $R_3^2 > R_4$ and $\sqrt{R_3^2 - R_4} > R_3$, and no real solution exists when $R_3^2 < R_4$. Equations (A17), (A15) and (A16) were solved iteratively with an accuracy of 10^{-8} to define steady state solution.

APPENDIX B: STABILITY ANALYSIS

B.1. SECOND ORDER STABILITY ANALYSIS USING TWO TERMS

Second order stability can be obtained by substituting

$$u(T) = A_1 \cos T + A_3 \cos 3T + B_3 \sin 3T + v(T) \tag{B1}$$

into equation (10); this leads to the following non-linear variational equation:

$$\ddot{v}\Omega^2 \left\{1 + \frac{\varepsilon_1}{2}(A_1^2 + A_3^2 + B_3^2 + (A_1^2 + 2A_1 A_3)\cos 2T + 2A_1 A_3 \cos 4T\right.$$
$$\left. + (A_3^2 + B_3^2)\cos 6T + 2A_1 B_3 (\sin 2T + \sin 4T) + 2A_3 B_3 \sin 6T)\right\}$$

$$+\dot{v}\{\delta\Omega+\varepsilon_1\Omega^2(2A_1B_3\cos 2T+4A_1B_3\cos 4T+6A_3B_3\cos 6T$$

$$-(A_1^2+2A_1A_3)\sin 2T-4A_1A_3\sin 4T+3(B_3^2-A_3^2)\sin 6T)\}$$

$$+v\left\{1+\frac{3}{2}\varepsilon_2(A_1^2+A_3^2+B_3^2)-\frac{\varepsilon_1}{2}\Omega^2(A_1^2+9A_3^2+9B_3^2)\right\}$$

$$+\left(\frac{3}{2}\varepsilon_2A_1^2+3\varepsilon_2A_1A_3-\frac{3}{2}\varepsilon_1\Omega^2A_1^2-7\varepsilon_1\Omega^2A_1A_3\right)\cos 2T$$

$$+(3\varepsilon_2A_1A_3-13\varepsilon_1\Omega^2A_1A_3)\cos 4T$$

$$+\left(\frac{1}{2}(3\varepsilon_2(A_3^2-B_3^2)-27\varepsilon_1\Omega^2(A_3^2+B_3^2))\right)\cos 6T$$

$$+(3\varepsilon_2A_1B_3-7\varepsilon_1\Omega^2A_1B_3)\sin 2T+(3\varepsilon_2A_1B_3-13\varepsilon_1\Omega^2A_1B_3)\sin 4T$$

$$+(3\varepsilon_2A_3B_3-27\varepsilon_1\Omega^2A_3B_3)\sin 6T+NLTS=0, \tag{B2}$$

where $NLTS$ stands for the non-linear terms, the second order stability is obtained by substituting

$$v(T)=b_0+b_{2c}\cos 2T+b_{2s}\sin 2T+b_{4c}\cos 4T+b_{4s}\sin 4T \tag{B3}$$

into the linearized version of equation (B2), and applying the harmonic balance; this leads to a set of linear homogeneous equations for b_0, b_{2c}, b_{2s}, b_{4c} and b_{4s}, that cas be written in matrix form as

$$\mathbf{Mb}=\mathbf{0}, \tag{B4}$$

where $\mathbf{b}$ is the column vector $(b_0, b_{2c}, b_{2s}, b_{4c}, b_{4s})^{\mathrm{T}}$ and $\mathbf{M}$ is the characteristic matrix. The elements of the coefficient matrix $\mathbf{M}$ are specified below:

$$M_{11}=1+\tfrac{3}{2}\varepsilon_2(A_1^2+A_3^2+B_3^2)-\tfrac{1}{2}\varepsilon_1\Omega^2\ (A_1^2+9A_3^2+9B_3^2),$$

$$M_{12}=\tfrac{1}{2}A_1B_3(3\varepsilon_2-7\varepsilon_1\Omega^2),$$

$$M_{13}=\tfrac{3}{4}\varepsilon_2(A_1^2+6A_1A_3)-\tfrac{1}{4}\varepsilon_1\Omega^2(3A_1^2+17A_1A_3),$$

$$M_{14}=\tfrac{1}{2}A_1B_3(3\varepsilon_2-13\varepsilon_1\Omega^2),$$

$$M_{15}=\tfrac{1}{2}A_1A_3(3\varepsilon_2-13\varepsilon_1\Omega^2),$$

$$M_{21}=\frac{\varepsilon_2}{2}(3A_1^2+6A_1A_3)-\tfrac{1}{2}\varepsilon_1\Omega^2(3A_1^2+14A_1A_3),$$

$$M_{22}=2\Omega\delta+\tfrac{1}{2}A_1B_3(3\varepsilon_2-9\varepsilon_1\Omega^2),$$

$$M_{23}=1-4\Omega^2+\tfrac{1}{2}\varepsilon_2(A_1^2+A_1A_3+A_3^2+B_3^2)-\tfrac{1}{2}\varepsilon_1\Omega^2(5A_1^2+9A_1A_3+13A_3^2+13B_3^2),$$

$$M_{24} = \tfrac{1}{2} B_3 (3\varepsilon_2 (A_1 + A_3) - \varepsilon_1 \Omega^2 (15A_1 + 19A_3)),$$

$$M_{25} = \tfrac{1}{4} \varepsilon_2 (3A_1^2 + 6A_1A_3 + 3A_3^2 - 3B_3^2) - \tfrac{1}{4} \varepsilon_1 \Omega^2 (11A_1^2 + 30A_1A_3 + 19A_3^2 - 19B_3^2),$$

$$M_{31} = A_1 B_3 (3\varepsilon_2 - 7\varepsilon_1 \Omega^2),$$

$$M_{32} = 1 - 4\Omega^2 + \tfrac{3}{2} \varepsilon_2 (A_1^2 - A_1A_3 + A_3^2 + B_3^2) - \tfrac{1}{2} \varepsilon_1 \Omega^2 (5A_1^2 - 9A_1A_3 + 13A_3^2 + 13B_3^2),$$

$$M_{33} = \tfrac{1}{2} A_1 B_3 (3\varepsilon_2 - 9\varepsilon_1 \Omega^2) - 2\Omega\delta,$$

$$M_{34} = \tfrac{1}{4} \varepsilon_2 (3A_1^2 + 6A_1A_3 - 3A_3^2 + 3B_3^2) - \tfrac{1}{4} \varepsilon_1 \Omega^2 (11A_1^2 + 15A_1A_3 - 19A_3^2 + 19B_3^2),$$

$$M_{35} = \tfrac{1}{2} B_3 (3\varepsilon_2 (A_3 - A_1) + \varepsilon_1 \Omega^2 (15A_1 - 19A_3)),$$

$$M_{41} = A_1 A_3 (3\varepsilon_2 - 13\varepsilon_1 \Omega^2),$$

$$M_{42} = \tfrac{1}{2} B_3 (3\varepsilon_2 (A_3 - A_1) + \varepsilon_1 \Omega^2 (15A_1 - 19A_3)),$$

$$M_{43} = \tfrac{1}{4} \varepsilon_2 (3A_1^2 + 6A_1A_3 + 3A_3^2 - 3B_3^2) - \tfrac{1}{4} \varepsilon_1 \Omega^2 (11A_1^2 + 15A_1A_3 + 19A_3^2 - 19B_3^2),$$

$$M_{44} = 4\Omega\delta,$$

$$M_{45} = 1 - 16\Omega^2 + \tfrac{3}{2} \varepsilon_2 (A_1^2 + A_3^2 + B_3^2) - \tfrac{1}{2} \varepsilon_1 \Omega^2 (17A_1^2 + 25A_3^2 + 25B_3^2),$$

$$M_{51} = A_1 B_3 (3\varepsilon_2 - 13\varepsilon_1 \Omega^2),$$

$$M_{52} = \tfrac{1}{4} \varepsilon_2 (3A_1^2 + 6A_1A_3 - 3A_3^2 + 3B_3^2) - \tfrac{1}{4} \varepsilon_1 \Omega^2 (11A_1^2 + 15A_1A_3 - 19A_3^2 + 19B_3^2),$$

$$M_{53} = \tfrac{1}{2} B_3 (3\varepsilon_2 (A_1 + A_3) - \varepsilon_1 \Omega^2 (15A_1 + 19A_3)),$$

$$M_{54} = 1 - 16\Omega^2 + \tfrac{3}{2} \varepsilon_2 (A_1^2 + A_3^2 + B_3^2) - \tfrac{1}{2} \varepsilon_1 \Omega^2 (17A_1^2 + 25A_3^2 + 25B_3^2),$$

$$M_{55} = -4\Omega\delta.$$

Non-trivial solutions for b_0, b_{2c}, b_{2s}, b_{4c} and b_{4s} exist only when the determinant of the coefficient matrix **M** in equation (B4) vanishes, which gives the second unstable portions of the steady state response curves of the non-linear oscillator obtained using two terms.

B.2. STABILITY ANALYSIS OF THE ASYMMETRIC SOLUTION

By following the above procedure, i.e., by substituting equation (31) into the LVE (30) and writing the set of linear algebraic equations in a matrix form, the elements of the characteristic matrix are

$$M_{11} = 1 - \frac{\Omega^2}{4} + 3\varepsilon_2 \left(A_0^2 - A_0A_1 + \frac{A_1^2}{2} \right) - \frac{\varepsilon_1 \Omega^2}{8} (2A_0^2 - 6A_0A_1 + 5A_1^2),$$

$$M_{21} = -\frac{\Omega\delta}{2},$$

$$M_{12} = \frac{\Omega\delta}{2},$$

$$M_{22} = 1 - \frac{\Omega^2}{4} + 3\varepsilon_2\left(A_0^2 + A_0A_1 + \frac{A_1^2}{2}\right) - \frac{\varepsilon_1\Omega^2}{8}(2A_0^2 + 6A_0A_1 + 5A_1^2),$$

Non-trivial solutions for $b_{1/2)c}$, $b_{1/2)s}$ exist only when the determinant of the coefficient matrix **M** vanishes, which gives the unstable portions of the asymmetric solution of the non-linear oscillator obtained using equations (28) and (29).